

# Morphology and electron-irradiation behaviour of poly(dimethyl silylene)

Andrew J. Lovinger, Frank J. Padden Jr and Don D. Davis

AT&T Bell Laboratories, Murray Hill, NJ 07974, USA

(Received 20 August 1990; revised 13 December 1990; accepted 13 December 1990)

We have obtained and studied the first single crystals of the important silicon-backbone polymer, poly(dimethyl silylene) (PDMS), by dissolution in  $\alpha$ -chloronaphthalene at 251°C and growth at 238°C. The crystals consist of molecularly folded, rhombic-shaped lamellae, analogous to those of carbon-based polymers. Electron diffraction patterns revealed a weak positional disorder in the intermolecular packing along the *b* crystallographic axis. The sensitivity of PDMS to electron irradiation was found to be substantially higher than that of typical polymers (e.g. polyethylene), with early structural changes seen at doses as low as 6 C m<sup>-2</sup>. By examining changes in composite electron diffraction reflections with radiation dose, we obtained evidence for two competing mechanisms in PDMS and showed that chain scission is much more extensive than crosslinking.

(Keywords: morphology; irradiation; poly(dimethyl silylene); structure; polysilanes)

## INTRODUCTION

Poly(dimethyl silylene) (PDMS) has been the object of increasing recent attention as the lowest homologue of the family of di-*n*-alkyl-substituted polysilylenes, (R<sub>2</sub>Si)<sub>*n*</sub>. These silicon-backbone polymers are also known as polysilanes, and the two terms will be used interchangeably here. The interest in these silicon-based polymers is centred both on their potential and actual applications, as well as on the fundamental aspects of their structures and properties. As regards applications, polysilanes are under intense examination as photoconducting<sup>1</sup>, electro-optic<sup>2</sup> or resist<sup>3</sup> materials, while PDMS itself is already a commercialized ceramic precursor for silicon carbide fibres<sup>4</sup>. With respect to structure and properties, the major interest in these materials lies in their thermo-chromism<sup>5-7</sup> and piezochromism<sup>8</sup>, as well as in the relative roles of the side chains *versus* the backbone in affecting the molecular conformation and solid-state transitions<sup>9-11</sup>.

We and our colleagues have been investigating the structures and phase transitions of these symmetrically substituted polysilylenes as a function of side-chain length<sup>5-12</sup>. In this context, PDMS is of primary interest, because the influence of the side chains is now minimized. In fact, its side groups are not chain-like as in the other homologues studied (e.g. diethyl to di-*n*-hexyl) but rather spherical-like, and their only motional freedom is rotation about the Si-C bond. They therefore do not have the ability to undergo side-chain crystallization, which can lead to very tight packings (akin to those of low molecular weight hydrocarbons) and cause record-high rigidities in the silicon backbone<sup>6</sup>, and which has been invoked energetically as the major conformational determinant for some of these polysilanes<sup>9</sup>.

Very recently<sup>11</sup>, we showed that the molecular conformation adopted by PDMS in the solid state is all-*trans*. *Trans* (or *trans*-like) arrangements had also recently been predicted as the lowest-energy conformations for PDMS both from an *ab initio* approach<sup>13</sup> and

from molecular mechanics or molecular orbital calculations<sup>14,15</sup>. Adoption of the *trans* conformation in PDMS points to the leading role of the silicon backbone in determining an intramolecular structure that maximizes the silicon  $\sigma$ -bond electron delocalization. In our previous study<sup>11</sup>, we also examined the molecular mobility, interchain packing and thermally induced phase transformations of this polymer.

Nevertheless, even though techniques for synthesis of PDMS have been known for a long time<sup>16,17</sup>, its crystallization and morphology have not been studied. This may be a result of its insolubility at temperatures below ~215°C<sup>17</sup>. In this work, we have examined single crystals and crystalline aggregates grown from  $\alpha$ -chloronaphthalene at temperatures in the region of 230-240°C, and also report on their behaviour under the effects of electron irradiation.

## EXPERIMENTAL

The sample of PDMS was synthesized as described previously<sup>11</sup>. Single crystals were grown by dissolution in  $\alpha$ -chloronaphthalene at 251°C to yield a 0.005% w/w solution, followed by slow cooling to 238°C and subsequent crystallization at this temperature. Polycrystalline aggregates were also obtained from such solutions by transferring the solution to ambient temperature from 251°C.

Drops of the suspension were deposited onto freshly cleaved mica and the solvent was evaporated in a vacuum oven for a few days. The dried crystals were then shadowed with Pt/C at a nominal angle of 26.5° and then coated with amorphous carbon in a vacuum evaporator. After flotation of the carbon film and crystals in water and deposition onto copper grids, the specimens were examined by conventional or scanning transmission electron microscopy and selected-area electron diffraction at 100 keV.

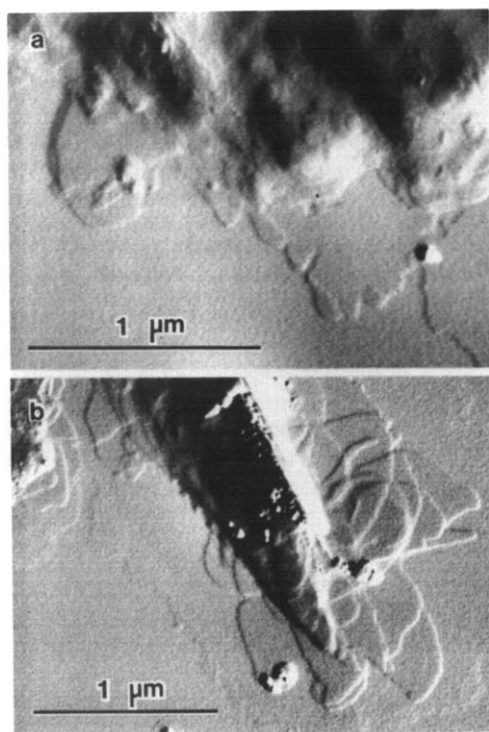


**Figure 1** Scanning transmission electron micrographs showing growth tips of PDMS spherulitic aggregates crystallized from 0.005% solution in  $\alpha$ -chloronaphthalene by cooling from 251 °C to ambient

## RESULTS AND DISCUSSION

When PDMS is crystallized from solution by cooling to ambient temperatures, it forms ill-defined multilayer aggregates that resemble immature spherulites. The growth tips of two such aggregates are seen in *Figure 1*. The situation in *Figure 1a* is the more typical one, i.e. one not exhibiting any macroscopic spherulitic fibrosity or elongated lamellae. The more radially elongated assembly seen in *Figure 1b* represents a rarer morphology. Even there, however, the individual lamellae are short and mutually misoriented, so that no clear preferred growth direction could be determined for these aggregates. Reasons for these features are attributed to very high nucleation of the polymer as the solution is cooled: we found the window between dissolution and cloud points for PDMS to be only  $\sim 15^\circ\text{C}$ .

In contrast to this very irregular morphology, highly regular single crystals and multilayers can be obtained by slow crystallization at very high temperatures (238 °C), as seen in *Figure 2*. The typical morphology consists of rhombic lamellae bounded by  $(1\ 1\ 0)$  growth facets and exhibiting profuse screw dislocations (*Figure 2a*). From their shadowing lengths, these lamellae are estimated to be only 6–9 nm thick. The  $a$  and  $b$  crystallographic axes correspond closely to the long and short diagonals of the rhombic lamellae. Small and commonly poorly developed  $(1\ 0\ 0)$  facets are also occasionally seen. More intricate geometries have also been observed (*Figure 2b*). These include dislocations of opposite hand leading to mutual annihilation, interpenetrating crystals and twinned lamellae.

It is thus seen that these silicon-backbone polymers crystallize with a thin, lamellar habit totally analogous to that of their carbon-based counterparts. We have shown previously<sup>18</sup> that in the case of poly(di- $n$ -hexyl

silylene) very thick ( $\sim 100$  nm) crystals are obtained, consisting of largely extended chains; because their molecular weights were several hundred thousand, these chains must not have been totally extended but folded a few times. As regards PDMS polymers, molecular weights are not known with certainty because of their insolubility below  $\sim 210^\circ\text{C}$ ; nevertheless, from infra-red and end-group analysis, molecular weights of the order of tens of thousands were estimated<sup>17</sup>. Moreover, our PDMS specimens exhibit an ultraviolet (u.v.) absorption peak at longer wavelengths (340 nm)<sup>11</sup> than found by Trefonas *et al.*<sup>19</sup>, indicating a degree of polymerization substantially higher than 40–50. In fact, this  $\lambda_{\text{max}}$  is much higher than the limiting value of the absorption peak wavelength ( $\sim 310$  nm) found for chains with  $>1000$  monomeric units<sup>19</sup>. Therefore, based also upon the thickness of our PDMS crystals and upon the fact that the molecules are oriented perpendicular to the broad lamellar surfaces (see below), we conclude that these silicon-backbone chains must be folded several times.

A typical electron diffraction pattern from PDMS single crystals is seen in *Figure 3*. The pattern consists of  $(h\ k\ 0)$  reflections with apparent systematic absences for  $h+k=2n+1$ . As described in a previous publication<sup>11</sup>, splitting in some reflections on X-ray diffractograms of PDMS suggested a very slight departure from an orthorhombic structure ( $\gamma=91^\circ$ ). The obvious first question from our single-crystal electron diffraction patterns is whether there is support for such a monoclinic packing. Unfortunately, there is no unambiguous answer. On the one hand, we find very slight deviations ( $\leq 1^\circ$ )

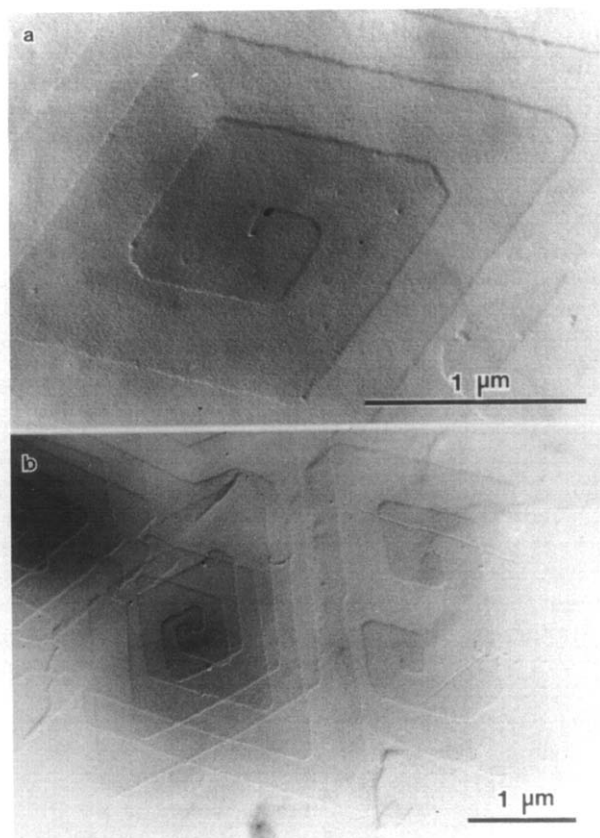


**Figure 2** Transmission electron micrographs showing typical morphologies of PDMS single crystals grown from 0.005% solution in  $\alpha$ -chloronaphthalene by slow cooling from 251 to 238 °C followed by isothermal crystallization at 238 °C

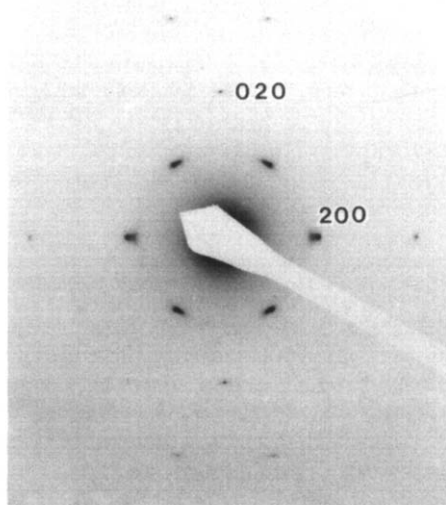


Figure 3 Typical selected-area electron diffraction pattern from a single crystal of PDMS

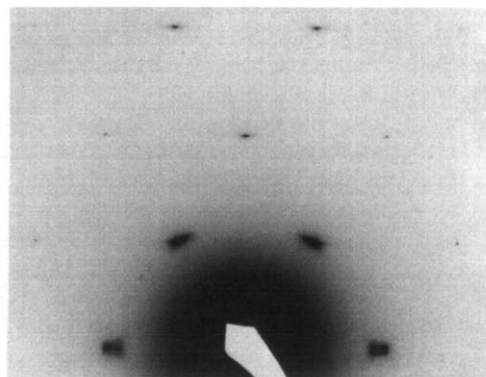


Figure 4 Detail of the  $k=0-3$  layers of the electron diffraction patterns from single crystals of PDMS showing the observed streaking along  $a^*$

from orthogonality of the  $a^*$  and  $b^*$  axes in our  $(h k 0)$  diffraction patterns. On the other hand, these are complicated by the fact that most reflections show a distinct streaking, and there are small but continuous shifts during electron irradiation as a result of the high beam sensitivity of this material (both of these aspects will be discussed presently). Moreover, systematic absences of the odd  $h+k$  reflections are not consistent with any of the general monoclinic space groups. If there is indeed a  $\leq 1^\circ$  departure from orthorhombic symmetry, perhaps the additional reflections are too weak to be detected or additional special symmetry elements are present, but this issue is still inconclusive.

Another feature of these  $(h k 0)$  single-crystal patterns from PDMS is the existence of a weak but long and distinct streak observed parallel to the  $a^*$  direction (Figure 4). It is noteworthy that this streak extends through all the upper-layer reflections, but that the  $(h 0 0)$  layer is unstreaked. This implies a positional disorder in the intermolecular placement of the PDMS chains along the  $b$  axis of the unit cell. A very similar effect was seen in the packing of the molecular chains of syndiotactic polypropylene<sup>20-22</sup>. However, in that polymer the streaking (and disorder) was generally more pronounced and increased greatly with undercooling<sup>22</sup>.

Additionally, the stable packing in syndiotactic polypropylene was not  $C$ -centred as here, but had all molecules on the edges of the unit cell<sup>21,22</sup>.

Another important aspect of the electron diffraction data from single crystals of PDMS is the fine structure of the  $(1 1 0)$  and  $(2 0 0)$  reflections. Figure 4 reveals irregular features in both, i.e. the  $(1 1 0)$  spots are clearly more arced than any of the other reflections, whereas the  $(2 0 0)$  appear to be composite peaks. Both of these characteristics can be probed in detail by examining the evolution of the diffraction pattern during observation in the electron microscope (i.e. as a function of radiation dose). This is done in Figure 5. Figure 5a is the original  $(h k 0)$  diffraction pattern, while Figure 5b was recorded from the same crystal after further electron irradiation.

By comparing these two figures, it is seen that the  $(1 1 0)$  reflections are not inherently arced but are in fact composites of a sharp, circular spot and of a diffuse, arced peak. The same is also true for the  $(2 0 0)$ , but here the arced component is located further 'inward' toward the main beam (i.e. at a higher  $d$ -spacing) and is initially almost imperceptibly weak in intensity. Figure 5b also shows that the diffuse, arced spots from the  $(2 0 0)$  and  $(1 1 0)$  peaks are disposed hexagonally to each other.

Additional important features of the  $(2 0 0)$  and  $(1 1 0)$  reflections are observed more clearly at the much

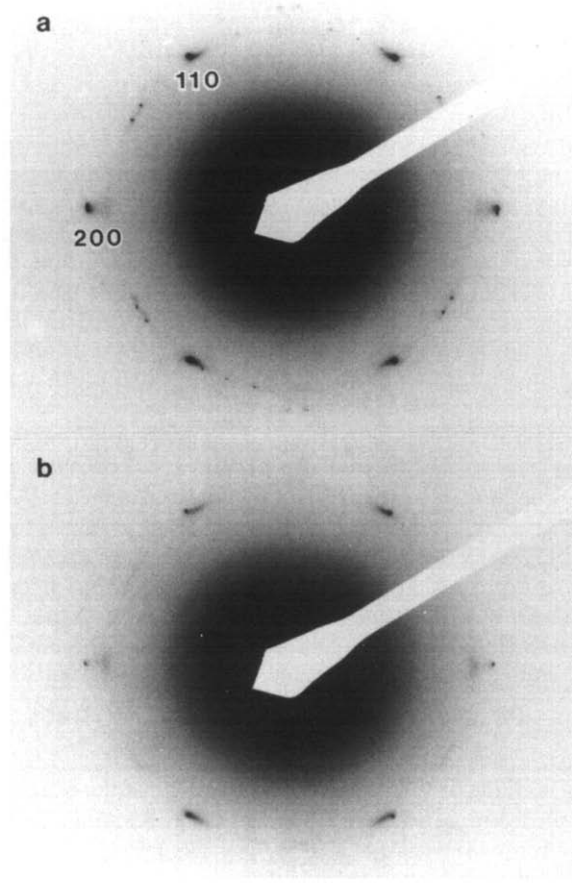
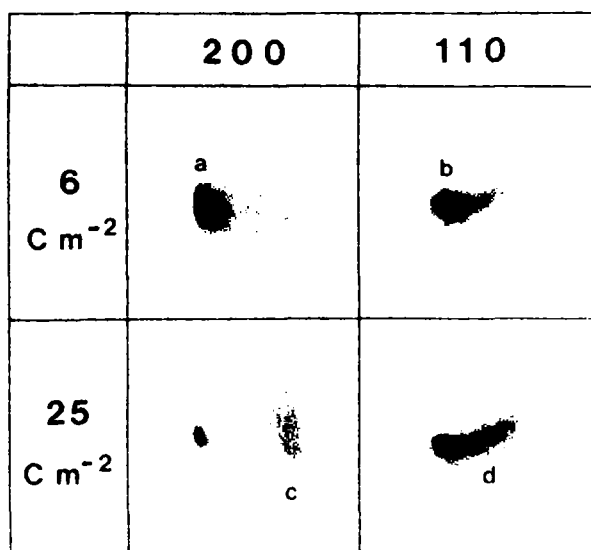


Figure 5 Successive selected-area electron diffraction patterns from a single crystal of PDMS recorded at average electron doses of (a)  $6 \text{ C m}^{-2}$  and (b)  $25 \text{ C m}^{-2}$



**Figure 6** Enlargement of the (2 0 0) and (1 1 0) reflections marked in Figure 5, showing the phase changes occurring as a result of electron irradiation

higher magnification of Figure 6, which also includes the average electron doses corresponding to each irradiation stage. From this figure it is seen that the original sharp spots ((a) and (b)) are greatly reduced in intensity, but retain their sharpness; they also do not shift in terms of reciprocal spacing. At the same time, the arced, diffuse reflections ((c) and (d)) observed at 25 C m<sup>-2</sup> are also present initially but at much smaller intensity. Additionally, the 25 C m<sup>-2</sup> photographs demonstrate that, for the (1 1 0) set the arced component changes substantially in azimuthal location, but only minimally in *d*-spacing compared to its sharp counterpart. The opposite is seen for the (2 0 0) peak, where the diffuse reflection is at a much higher interplanar spacing but same equatorial disposition as the original, sharp spot.

All of these features of the diffuse (2 0 0) and (1 1 0) components are entirely consistent with a crosslinking mechanism for electron-induced radiation damage in PDMS. Such irradiation is well known to lead to an expanded, defective, quasi-hexagonal packing of the chains (on the road to full amorphization by extensive crosslinking) for most crystalline polymers, as typified by polyethylene<sup>20</sup>. However, PDMS is seen to be more sensitive to these effects of electron irradiation. The first indications of a transformation to such a defective, quasi-hexagonal packing are already visible at 6 C m<sup>-2</sup> (Figure 6) and the reflections merge to an amorphous-like halo at ~40–50 C m<sup>-2</sup>. For the more typical case of polyethylene<sup>21</sup>, amorphization is observed at ~100 C m<sup>-2</sup>, while for polymers containing  $\pi$ -conjugated groups [as in, e.g. poly(*p*-phenylene sulphide)]<sup>22</sup> the corresponding dose can be tens of times greater<sup>23,24</sup>. It may seem remarkable that the  $\sigma$  conjugation of these silicon-backbone polymers does not have a similar effect, but the Si–Si bond is, of course, well known to be radiolytically<sup>25</sup> and photolytically<sup>26</sup> highly unstable.

While crosslinking accounts for the emergence and evolution of the broad, arced reflections during electron irradiation of PDMS, the behaviour of the strong, sharp spots requires a different mechanism. From Figure 6, this behaviour involves preservation of the shape, sharpness and reciprocal-space location of these reflections, but

with continuously decreasing intensity. Thus, while the lattice disruptions from crosslinking are representative of distortions of the second kind (paracrystalline), those seen in the sharp spots are typical of distortions of the first kind (quasi-thermal), where the near-neighbour relationships are disturbed but the long-range lattice order remains<sup>21</sup>. However, the molecular origins of such effects on the sharp reflections may lie in one of two possible mechanisms: crosslinking with phase separation or chain scission.

The first of these is typified by paraffinic hydrocarbons and has been studied extensively by Ungar *et al.*<sup>27,28</sup>. They showed that such paraffins undergo phase separation between crosslinked and undamaged areas: the crosslinked regions were distinctly visible in bright-field electron microscopic images as non-diffracting 'droplets'<sup>28</sup>. The second molecular origin leading to the observed decrease of reflection intensities without change in profile or location is chain scission, described most commonly for polyoxymethylene<sup>20,21,29</sup>.

Of these two possible mechanisms, chain scission clearly seems to be the appropriate one for PDMS. No formation, growth and coalescence of droplet-like regions was observed in our specimens. Moreover, chain scission has been extensively documented in polysilanes<sup>25</sup> and lower homologues<sup>26,30</sup>, and is in fact the basis for their potential application as positive u.v.- and electron-beam resists<sup>25</sup>. Such chain scission has been explicitly shown<sup>25</sup> to occur radiolytically under conditions extremely similar to ours, i.e. by  $\gamma$  irradiation (<sup>60</sup>Co) under vacuum.

We thus conclude that the combined electron diffraction changes observed during irradiation of PDMS arise from a coexistence of two competing processes—chain scission and crosslinking. The relative extents of these two reactions depend upon the individual susceptibilities of main chain *versus* side group bond cleavage, the nature and reactivity of the intermediates, the rates of chain diffusion and recombination, as well as on cage effects in the crystalline phase. In considering the relative tendencies toward chain scission *versus* crosslinking in our own samples and under our own experimental conditions, we may examine densitometric scans through the composite (2 0 0) and (1 1 0) reflections as a measure of intensity change during electron irradiation. Such traces are presented in Figure 7. We see for both the (2 0 0) and (1 1 0) scans that the reduction in the intensity of the strong, sharp peak after an increase in electron dose is much greater than the corresponding growth in the weak, broad peak. These measurements must be taken with caution because of saturation and non-linearity effects of the film and photodetector at high intensities. However, these effects would tend to attenuate preferentially the intensities of the strong, scission-associated peaks and therefore underestimate the extent of this process relative to crosslinking.

Support for the primacy of chain scission over crosslinking in our specimens is also provided by the behaviour of other symmetrically substituted polysilylenes. For the di-*n*-butyl and di-*n*-hexyl homologues, Miller<sup>25</sup> reports the relative rates of scission, *G*(s), and crosslinking *G*(x), under  $\gamma$  irradiation; these are defined as the numbers of chain scissions or crosslinks per 100 eV of absorbed dose. For both polymers, *G*(s) was 0.42, while *G*(x) was in the range of 0.02–0.04<sup>25</sup>. For

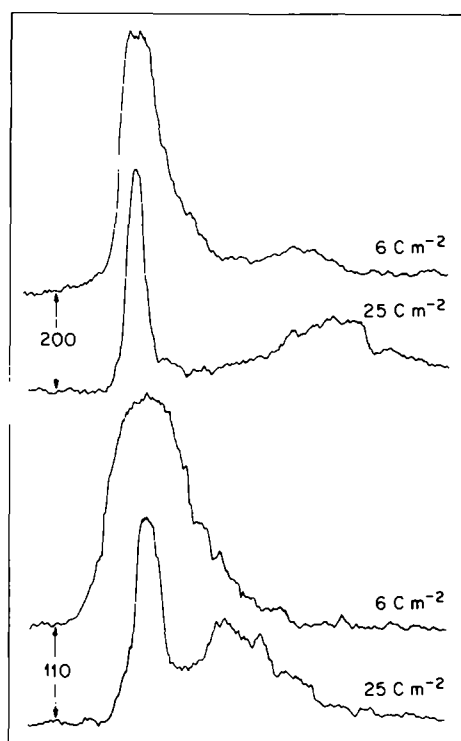


Figure 7 Densitometric traces (parallel to the  $a^*$  direction) through the (2 0 0) and (1 1 0) composite electron diffraction peaks of PDMS at two different radiation doses

comparison, polyethylene (which undergoes essentially pure crosslinking) has a  $G(x)$  of  $\sim 0.10$ , whereas PMMA (which is extremely susceptible to scission) has a  $G(s)$  of  $\sim 1.40$ .

#### ACKNOWLEDGEMENT

We are grateful to Dr J. M. Zeigler for providing the PDMS specimen used in this study.

#### REFERENCES

- 1 Kepler, R. G., Zeigler, J. M., Harrah, L. A. and Kurtz, S. R. *Phys. Rev. B* 1987, **35**, 2818
- 2 Zeigler, J. M., Harrah, L. A. and Johnson, A. W. *SPIE Adv. Resist Tech.* 1985, **537**, 166
- 3 Yang, L., Wang, Q. Z., Ho, P. P., Dorsinville, R., Alfano, R. R., Zou, W. K. and Yang, N. L. *Appl. Phys. Lett.* 1988, **53**, 1245
- 4 Yajima, S., Hayashi, J. and Omori, M. *Chem. Lett.* 1975, 931
- 5 Rabolt, J. F., Hofer, D., Miller, R. D. and Fickes, G. N. *Macromolecules* 1986, **19**, 611
- 6 Lovinger, A. J., Schilling, F. C., Bovey, F. A. and Zeigler, J. M. *Macromolecules* 1986, **19**, 2657, 2660
- 7 Kuzmany, H., Rabolt, J. F., Farmer, B. L. and Miller, R. D. *J. Chem. Phys.* 1986, **85**, 7413
- 8 Schilling, F. C., Bovey, F. A., Davis, D. D., Lovinger, A. J., Macgregor Jr, R. B., Walsh, C. A. and Zeigler, J. M. *Macromolecules* 1989, **22**, 4645
- 9 Farmer, B. L., Rabolt, J. F. and Miller, R. D. *Macromolecules* 1987, **20**, 1167
- 10 Lovinger, A. J., Davis, D. D., Schilling, F. C., Bovey, F. A. and Zeigler, J. M. *Polym. Commun.* 1989, **30**, 356
- 11 Lovinger, A. J., Davis, D. D., Schilling, F. C., Padden Jr, F. J., Bovey, F. A. and Zeigler, J. M. *Macromolecules* 1991, **24**, 132
- 12 Schilling, F. C., Lovinger, A. J., Zeigler, J. M., Davis, D. D. and Bovey, F. A. *Macromolecules* 1989, **22**, 3055
- 13 Mintmire, J. W. *Phys. Rev. B* 1989, **39**, 13350
- 14 Welsh, W. J. and Johnson, W. D. *Macromolecules* 1990, **23**, 1881
- 15 Cui, C. X., Karpfen, A. and Kertesz, M. *Macromolecules* 1990, **23**, 3302
- 16 Burkhard, C. A. *J. Am. Chem. Soc.* 1949, **71**, 963
- 17 Wesson, J. P. and Williams, T. C. *J. Polym. Sci., Polym. Chem. Edn* 1979, **17**, 2833
- 18 Schilling, F. C., Bovey, F. A., Lovinger, A. J. and Zeigler, J. M. *ACS Adv. Chem. Ser.* 1990, **224**, 341
- 19 Trefonas III, P. T., West, R., Miller, R. D. and Hofer, D. J. *J. Polym. Sci., Polym. Lett. Edn* 1983, **21**, 819
- 20 Grubb, D. T. *J. Mater. Sci.* 1974, **9**, 1715
- 21 Orth, H. and Fischer, E. W. *Makromol. Chem.* 1965, **88**, 188
- 22 Lovinger, A. J., Padden Jr, F. J. and Davis, D. D. *Polymer* 1988, **29**, 229
- 23 Tsuji, M., Roy, S. K. and St J. Manley, R. *J. Polym. Sci., Polym. Chem. Edn.* 1985, **23**, 1127
- 24 Kumar, S. and Adams, W. W. *Polymer* 1990, **31**, 15
- 25 Miller, R. D. *ACS Adv. Chem. Ser.* 1990, **224**, 413
- 26 Nate, K., Ishikawa, M., Imamura, N. and Murakami, V. *J. Polym. Sci., Polym. Chem. Edn.* 1986, **24**, 1551
- 27 Ungar, G. *Polymer* 1980, **21**, 1278
- 28 Ungar, G., Grubb, D. T. and Keller, A. *Polymer* 1980, **21**, 1284
- 29 Grubb, D. T. and Groves, G. W. *Phil. Mag.* 1971, **24**, 815
- 30 Ishikawa, M., Takaoka, T. and Kumada, M. *J. Organomet. Chem.* 1972, **42**, 333